$\sum_{\mathbf{k}} P(\mathbf{k}) = N$ and we choose the marginal distributions of the in-degrees and the out-degrees to be equal.

Using the theory in [16] (or see [15, 5] for similar derivations) one can show that the long-time dynamics of the network is described by

$$\frac{\partial b(\mathbf{k};t)}{\partial t} = \frac{R(\mathbf{k};t)}{2} + [i\omega_0(\mathbf{k}) - \Delta(\mathbf{k})]b(\mathbf{k};t) - \frac{R(\mathbf{k};t)}{2}[b(\mathbf{k};t)]^2 \tag{5}$$

where $\omega_0(\mathbf{k})$ and $\Delta(\mathbf{k})$ are the centre and half-width at half-maximum, respectively, of the Lorentzian distribution from which the values of ω_j for oscillators with degree $\mathbf{k}$ are chosen:

$$g(\omega(\mathbf{k})) = \frac{\Delta(\mathbf{k})/\pi}{[\omega(\mathbf{k}) - \omega_0(\mathbf{k})]^2 + \Delta^2(\mathbf{k})} \tag{6}$$

The variable

$$b(\mathbf{k};t) = \int_{-1}^{1}\int_{0}^{2\pi} f(\theta;\omega|\mathbf{k};t)e^{-i\theta}\,d\theta\,d\omega \tag{7}$$

is the complex-valued order parameter for oscillators with degree $\mathbf{k}$, where $f(\theta;\omega|\mathbf{k};t)\,d\theta\,d\omega$ is the probability that an oscillator with degree $\mathbf{k}$ has phase in $[\theta;\ \theta + d\theta]$ and frequency in $[\omega;\ \omega + d\omega]$ at time t. $R(\mathbf{k};t)$ is given by

$$R(\mathbf{k};t) = \frac{1}{\langle k\rangle i}\sum_{\mathbf{k}'} P(\mathbf{k}')a(\mathbf{k}' \to \mathbf{k})G(\mathbf{k}';t) \tag{8}$$

where

$$G(\mathbf{k};t) = 1 + \frac{4}{5}\left[\frac{b(\mathbf{k};t) + \bar{b}(\mathbf{k};t)}{2}\right] + \frac{b^2(\mathbf{k};t) + \bar{b}^2(\mathbf{k};t)}{2} + \frac{4}{35}\left[\frac{b^3(\mathbf{k};t) + \bar{b}^3(\mathbf{k};t)}{2}\right] + \frac{b^4(\mathbf{k};t) + \bar{b}^4(\mathbf{k};t)}{70} \tag{9}$$

where overline indicates the complex conjugate. The form of G is determined by the function $T(\ )$. This derivation of a degree-dependent mean field description uses the Ott/Antonsen ansatz [24, 25]. A crucial ingredient for the use of this ansatz is the sinusoidal form of the function $U(\ )$.

We are interested in the case of neutral assortativity, for which [31]

$$a(\mathbf{k}' \to \mathbf{k}) = \frac{k'_{out}k_{in}}{N\langle k\rangle} \tag{10}$$

and cases where either the in- and out-degree of an oscillator are independent, or they are equal (and thus perfectly correlated). Writing $P(k'_{in};k'_{out})$ instead of $P(\mathbf{k}')/N$ we have

$$R(k_{in};k_{out}) = \frac{k_{in}}{\langle k\rangle i^2}\sum$$

where g is the Lorentzian (6) and thus the mean firing rate over the network is

$$F = \frac{1}{2} \sum_{k_{in}} p(k_{in}) f(k_{in}) \tag{20}$$

For comparison with our results below we briefly describe the dynamics of a fully connected network of Winfree oscillators. Two types of behaviour are typically seen in such a network: synchronous and asynchronous [26, 7], although the fraction of oscillators actually oscillating varies in different asynchronous states. Increasing Δ tends to destroy synchronous behaviour through a saddle-node-on-invariant-circle (SNIC) bifurcation, as many of the oscillators "lock" to an approximate fixed point. For moderate Δ increasing the spread of intrinsic frequencies tends to destroy synchronous behaviour through a supercritical Hopf bifurcation, as the oscillators become too dissimilar in frequency to synchronise [26]. Below we will see a wider variety of bifurcations resulting from the networks' structure.

3. Gaussian frequency distribution

We choose the degree distribution $p(k)$ to be a truncated power law distribution with exponent -3, as many others have done when studying ES [18, 8]:

$$p(k) = \begin{cases} a/k^3 & m \le k \le M \\ 0 & \text{otherwise} \end{cases} \tag{21}$$

where a is a normalisation such that

$$\sum_{k=m}^{M} \frac{a}{k^3} = 1. \tag{22}$$

Since the degrees are all large (i.e. $1 \ll m$) we treat k as a continuous variable and approximate the sum in (22) by

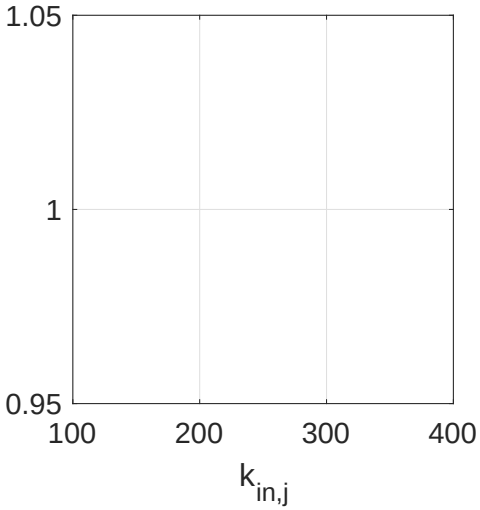

Figure 1. (a): solid line: (24); dots: target frequencies and degrees for one realisation of a network. (b): solid line: (24); dots: actual frequencies and degrees for one realisation of a network. Parameters: $m = 100$; $M = 400$; $N = 2000$; $= 0.01$; $= 0.00005$.

frequency with the node with smallest in-degree etc. These values are shown as dots in panel (a), along with the theoretical relationship (24). Panel (b) shows the actual values of the $!_j$ (dots), taken from a Lorentzian with centre equal to the values in panel (a) and HWHM 0.00005.

Clearly there is a positive correlation between $k_{in;j}$ and $!_j$, but the Pearson correlation coefficient between them, defined by

$$_{k!} = \frac{\sum_{j=1}^{N}(k_{in;j} - \langle k \rangle)(!_j - !)}{\sqrt{\sum_{j=1}^{N}(k_{in;j} - \langle k \rangle)^2}\sqrt{\sum_{j=1}^{N}(!_j - !)^2}} \tag{26}$$

where $!$ is the mean of the $!_j$, is less than 1 and (using this construction) cannot be systematically varied, as was possible in [16, 15]. Note that the idea of not having a perfect match between an oscillator's degree and a prescribed frequency (as we have here for $\sigma > 0$) was discussed in [33], where it was shown that such a mismatch actually *created* ES.

To investigate the influence of varying the correlation between $k_{in;j}$ and $!_j$, we created a sequence of the appropriate degrees, chose values of $!$ from a Gaussian distribution and randomly paired them. We then repeatedly performed Monte Carlo swaps of $!$ values; potential swaps were accepted if they increased the Pearson correlation coefficient toward a target value – typically a positive number. This approach required substantial effort to satisfy high correlations (≥ 0.9), since a sequence of $!$ randomly paired with degree sequences typically exhibited no correlation. Alternatively, we maximised the correlation between the $k_{in;j}$ and $!_j$ by initially sorting both sequences as above. Aligning maximal-minimal values then produced the highest possible correlation coefficient for given sequences which we then reduced using Monte Carlo swaps, with swaps accepted if they pushed the correlation value toward a target value. Sequences of degrees and frequencies generated with this approach were assembled into adjacency

matrices utilising our network assembly scheme, the \permutation method", presented previously [20]. Note that with this approach of constructing networks the Ott/Antonsen approach cannot be used, and we must simulate the resulting networks to determine their behaviour.

3.1. Results. We numerically investigate (16) with (14). We evaluate functions at all integer in-degrees satisfying $m + 1 \le k_{in} \le M - 1$ to avoid the singularities in ϕ^{-1} when its argument is either 0 or 1, resulting in a moderately large set of ordinary differential equations. We could use a more efficient method which approximates the sum in (14) with fewer \virtual" degrees as explained in [15], but that is unnecessary here. Typically we integrate (16) to a stable fixed point and then use pseudo-arclength continuation to follow the fixed point as parameters are varied, determining the stability of the fixed point from the eigenvalues of the linearisation of the dynamics about the fixed point [13, 9]. Periodic solutions are studied in a similar way by putting a Poincare section in the flow (at $\mathrm{Re}[b(m+1;t)] = 0$) and integrating from this section until the solution next hits this section. Stability is given by the Floquet multipliers of the periodic solution.

The usual complex-valued order parameter defined for the network (1) is

$$Y(t) = \frac{1}{N}\sum_{j=1}^{N} e^{i\theta_j} \tag{27}$$

and for (16) the appropriate measure is

$$Z(t) = \sum_{k_{in}} p(k_{in})b(k_{in};t) \tag{28}$$

We first vary with = 0:01. Results are shown in Fig. 2, where panel (a) shows results from (16). For small (16) has a stable fixed point at which the network is incoherent, with $|Z|$ being small. As is increased the fixed point undergoes a subcritical Hopf bifurcation, becoming unstable. (In the all-to-all coupled network, this Hopf bifurcation is supercritical.) The unstable periodic orbit created in this bifurcation is shown with red crosses and it becomes stable in a saddle-node bifurcation. Thus there is a small range of values for which the network is bistable. (For periodic orbits, the quantity plotted on the vertical axis is the average over one period of $|Z(t)|$.)

Panel (b) of Fig. 2 shows $|Y|$ for the network (1) with quasistatically increased or decreased, using the final state of the network at one value of as the initial condition for the next value. The value plotted is the mean over 5000 time units of $|Y(t)|$. The bistability and hysteresis is clear. Networks of the form used in (1) were created using the configuration model [

Figure 2. (a): $|Z|$ for fixed point (lines) and periodic solutions (symbols) of (16). Blue solutions are stable while red are unstable. (b): $|Y|$ for the network (1). Black corresponds to increasing and magenta to decreasing. Parameters: $m = 100$; $M = 400$; $N = 2000$; $= 0.01$; $= 0.0005$.

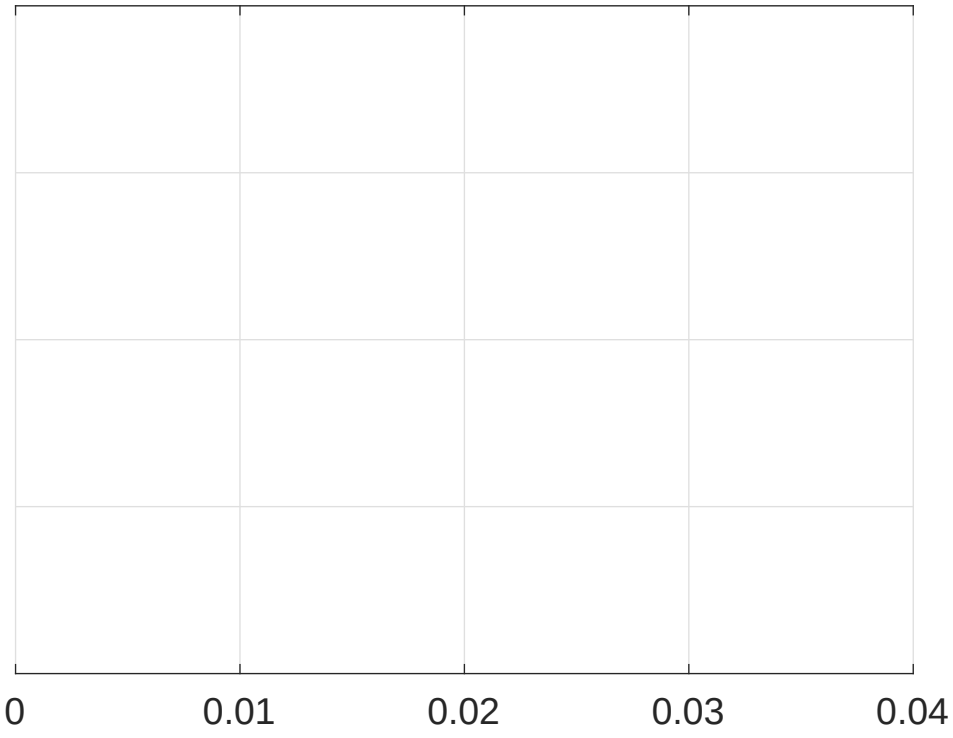

Figure 3. Curves of Hopf and saddle-node bifurcations as seen in Fig. 2(a) as both and are varied. The network is bistable between the curves. Parameters: $m = 100$; $M = 400$; $= 0.0005$.

quasistatically increased or decreased the coupling strength and measured the time-averaged value of $|Y|$. This is shown in Fig 4C where we see results similar to those in Fig. 2 | a small region of bistability. Panel D of Fig 4 shows the fraction of effective frequencies as the coupling strength is progressively increased, at $\sigma_\omega = 0.95$.

The distribution of frequencies and their fractional evolution corresponds to the mean and standard deviation of the Gaussian distribution, and the highest concentration of frequencies around the mean emerge dominant. However, the effects of having a large value of σ_ω for Gaussian distributed intrinsic frequencies is minimal compared with that for power law distributed frequencies, considered next.

4. Power law frequency distribution

We keep the power law distribution of degrees (21) and now consider the case where the target distribution frequency distribution is also power law distributed and limited between c and C, but with the exponent as a parameter, i.e.

$$p_{\omega_0}(\omega_0) = \begin{cases} a_\omega/\omega_0^{\gamma+1} & c \le \omega_0 \le C \\ 0 & \text{otherwise} \end{cases} \tag{29}$$

where $a_\omega = c^\gamma C^\gamma/(C^\gamma - c^\gamma)$. As above, having created a network we randomly choose target frequencies from the distribution (29), then assign the smallest target frequency to the oscillator with the smallest in-degree, all the way up to the largest target frequency being associated with oscillator with the largest in-degree. The actual ω_j are then chosen from a Lorentzian with HWHM equal to Δ centred at the target frequency, as above. The dependence of ω_0 on k is then

$$\omega_0(k) = \beta_{\omega_0}^{-1}(\beta(k)) \tag{30}$$

where β_{ω_0} is the cumulative distribution function of p_{ω_0}, i.e

$$\beta_{\omega_0}(\omega_0) = \frac{a_\omega}{\gamma}\left(\frac{1}{c^\gamma} - \frac{1}{\omega_0^\gamma}\right) \tag{31}$$

4.1. Highly correlated degree and frequency.

4.1.1. *Independent degrees.* We first consider the case of independent degrees, as in Sec. 3. Thus we numerically investigate (16) with (14), but using (30). We choose $\Delta = 0.01$, set $c = 1; C = 6$, and initially choose $K = 2$. As in Sec. 3, for small K the system has a stable fixed point and this becomes unstable through a subcritical Hopf bifurcation as K is increased. The results are shown in Fig. 5 where we see the periodic orbit created in the Hopf bifurcation, giving the same scenario as in Fig. 2 (a). Quasistatically increasing K the solution of (16) would jump from a fixed point to a periodic state with amplitude significantly larger than zero. Decreasing K, the solution would jump from a finite-amplitude periodic orbit to a fixed point. (As above, for periodic orbits, the quantity plotted on the vertical axis is the average over one period of $|Z(t)|$.)

The behaviour of a particular realisation of the discrete network (1) is slightly different, since a fixed point of (16) corresponds to an incoherent solution of (1) for which $|Y|$ is not constant, having small fluctuations about an average value. An example of such dynamics is shown in Fig. 6(a), with $K = 0.92$. (Other parameters have the same values as in Fig. 5.) We see that most oscillators are oscillating, but with independent phases. Similarly, a periodic solution of (16) corresponds to a solution of (1) for which $|Y|$ is nearly periodic, with the vast

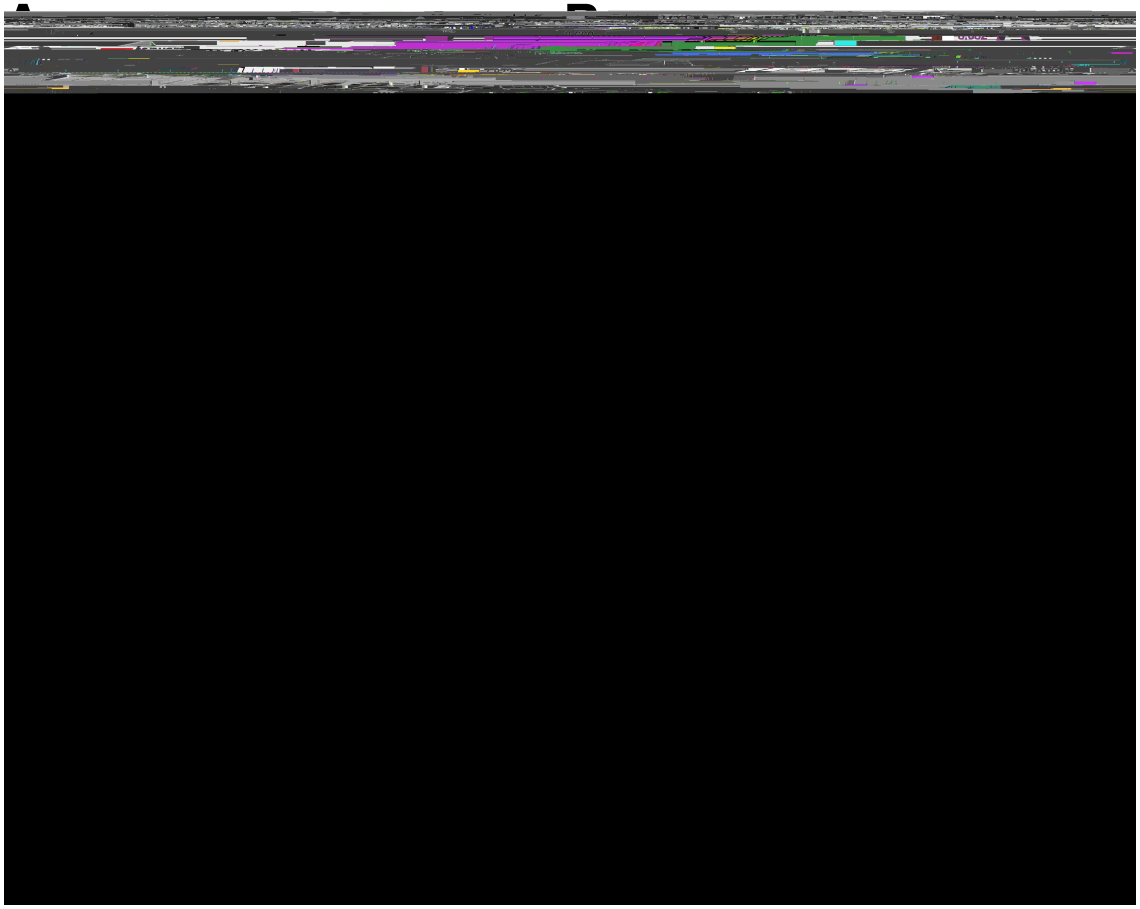

Figure 4. Panels A and C: $|Y|$ as σ is quasistatically varied for networks with different values of $k_!$. Panels B and D: Progression of mean-effective frequency fraction distribution over increasing coupling strength σ, for $k_!$ = 0.95; note

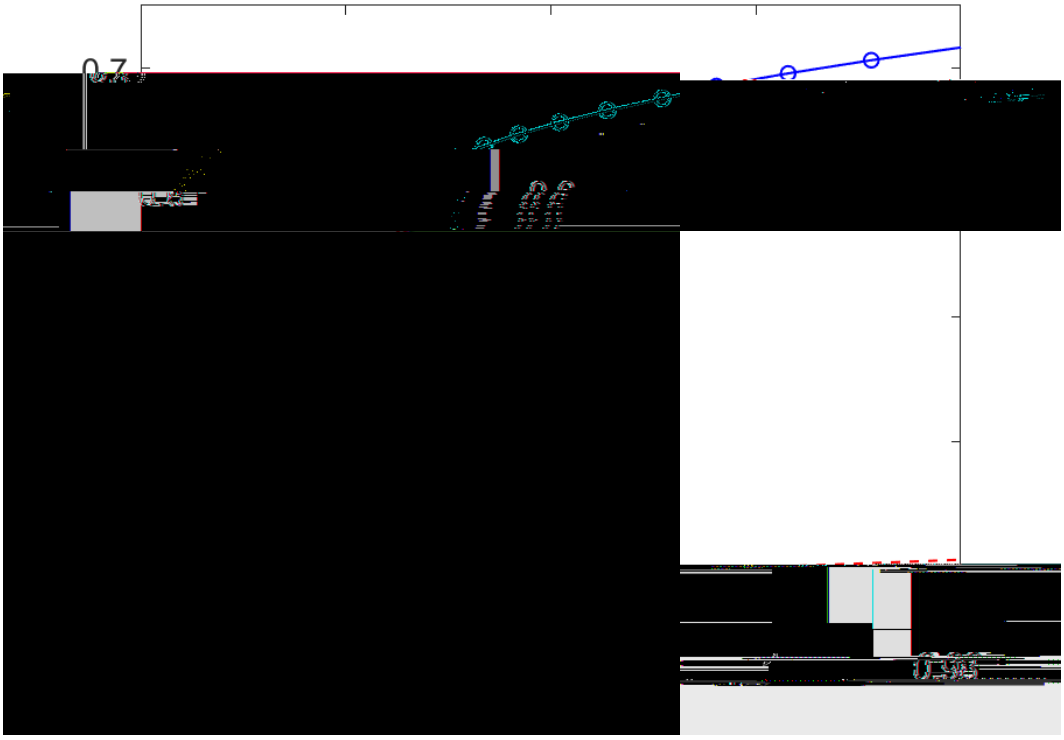

Figure 5. $|Z|$ for fixed point (lines) and periodic (symbols) solutions of (16). Blue solutions are stable while red are unstable. Parameters: $c = 1; C = 6; m = 100; M = 400; \quad = 2; \quad = 0.01$.

hypothesise that it is destroyed in a homoclinic bifurcation with the \middle" unstable branch. Thus the system has no stable periodic orbits, but rather a region of bistability between two fixed points with different values of $|Z|$. Either increasing or decreasing the network jumps from one fixed point to another. Fig. 7(b) shows the mean firing rate F across the network and we see that the branch with large $|Z|$ has small F and vice versa. So even if $|Z|$ is large, normally indicating synchronous oscillations, here it corresponds to a state in which most of the oscillators are locked at an approximate fixed point, not firing.

Fig. 8 shows (on a logarithmic scale) the expected frequency for oscillators with in-degree k_{in}, given by (19), for three coexisting steady states in Fig. 7 at $= 1.7$. The stable solution with highest frequencies has the lowest value of $|Z|$ and vice versa. Interestingly, for the upper curve the frequency increases with in-degree k_{in}, but for the lower two curves the maximum frequency does not occur at either extreme of the k_{in} values.

A third scenario occurs for $= 1.5$, as seen in Fig. 9. The fixed point that is stable for small becomes unstable through a subcritical Hopf bifurcation as is increased as in Fig. 5, but the stable periodic orbit is destroyed in a SNIC bifurcation which occurs at a slightly lower value of than that at which the Hopf bifurcation occurs. So if is slowly increased the network will jump from one fixed point to another fixed point. But if is then decreased the network will switch from a fixed point to a stable periodic orbit. This stable orbit is then destroyed in a saddle-node bifurcation as is further decreased and the network will jump to the original fixed point.

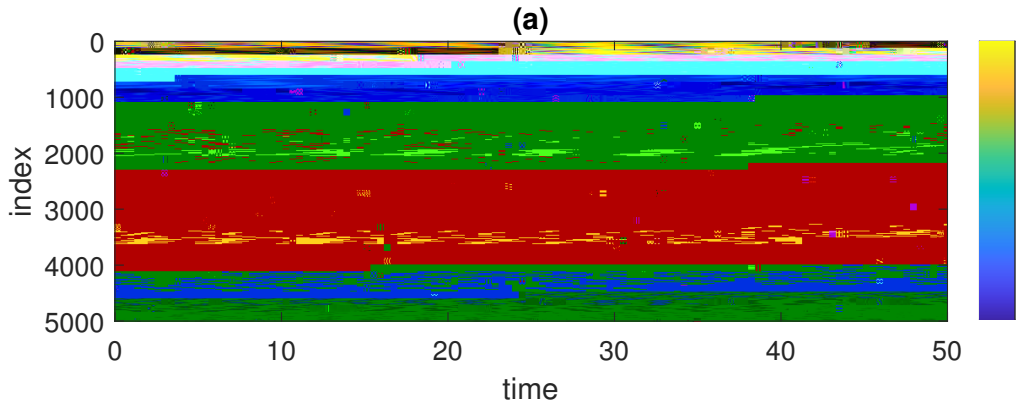

Figure 6. sin shown in colour for a simulation of (1). The oscillators are sorted by their in-degree. (a): = 0:92. (b): = 1. Other parameters: *N*

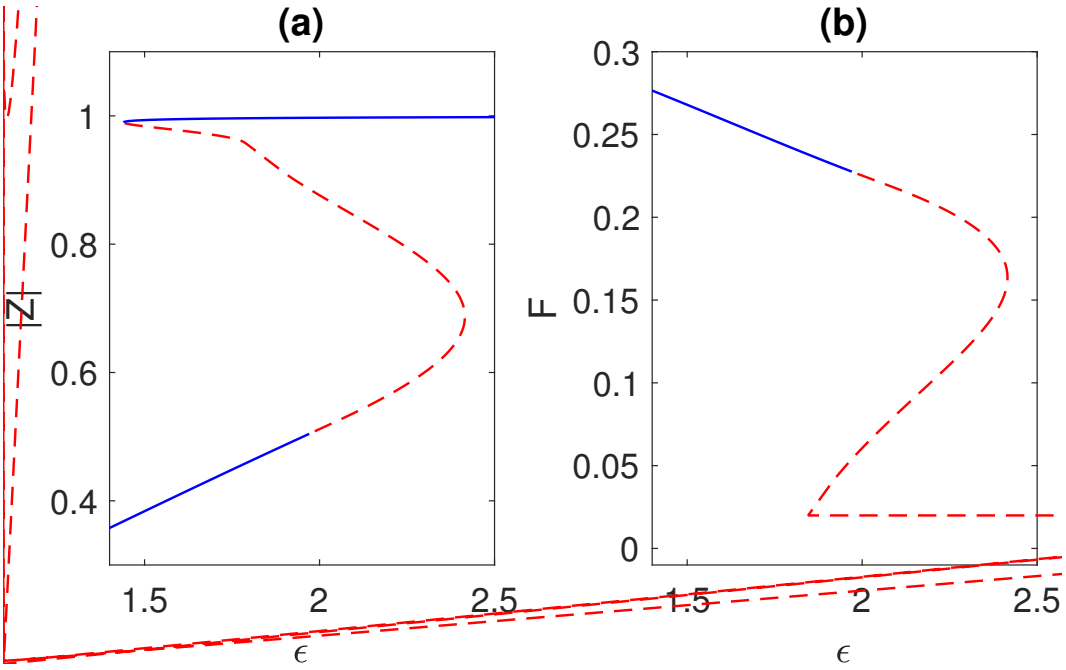

Figure 7. (a) jZj and (b) mean ring rate F for xed points of (16). Solid: stable; dashed: unstable. The bifurcation on the lower branch in (a) is a subcritical Hopf. Parameters: $c = 1; C = 6; m = 100; M = 400;$ $= 1;$ $= 0{:}01$.

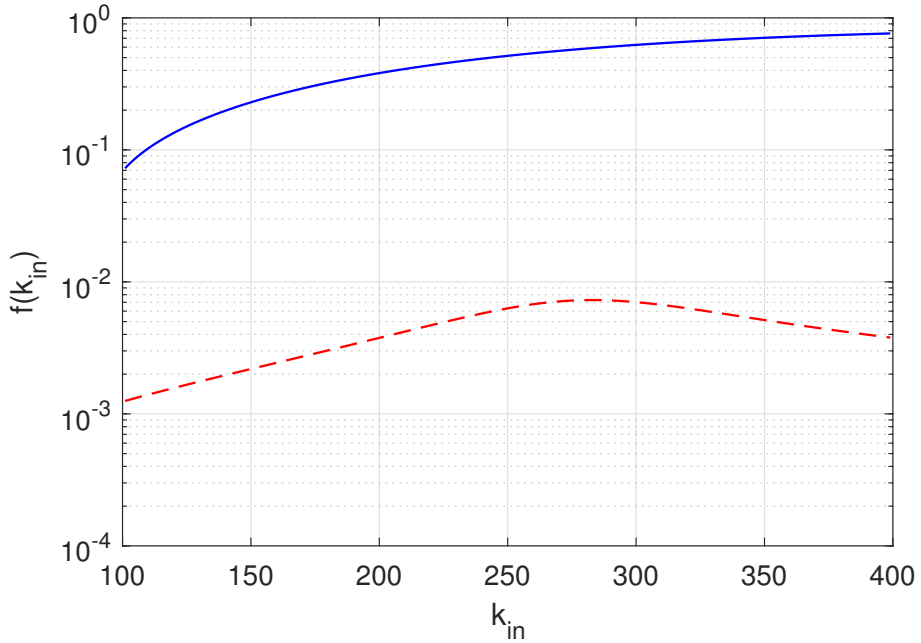

Figure 8. Expected frequency for oscillators with in-degree k_{in}, given by (19), for three coexisting steady states at $= 1{:}7$. See Fig. 7. Blue: stable solutions; red: unstable solution. Other parameters: $c = 1; C = 6; m = 100; M = 400;$ $= 1;$ $= 0{:}01$.

Figure 9. jZj for xed point (lines) and periodic (symbols) solutions of (16). Blue solutions are stable while red are unstable. The stable branch of periodic orbits terminates at the SNIC bifurcation. Parameters: $c = 1; C = 6; m = 100; M = 400; \quad = 1{:}5; \quad = 0{:}01$.

Figure 10. Identical degrees. $|Z|$ for fixed point (lines) and periodic (symbols) solutions of (16). Blue solutions are stable while red are unstable. The stable branch of periodic orbits terminates at the SNIC bifurcation. Parameters: $c = 1; C = 6; m = 100; M = 400; \quad = 2; \quad = 0.01$.

Figure 11.

[14] Carlo R Laing. E ects of degree distributions in random networks of type-i neurons. *Physical Review E*, 103(5):052305, 2021.

[15] Carlo R Laing and Christian Bla sche. The e ects of within-neuron degree correlations in networks of spiking neurons. *Biological Cybernetics*, 114:337{347, 2020.

[16] Carlo R Laing, Christian Bla sche, and Shawn Means. Dynamics of structured networks of winfree oscillators. *Front Syst Neurosci*, 15:631377, 2021.

[17] I Leyva, A Navas, I Sendina-Nadal, JA Almendral, JM Buldu, M Zanin, D Papo, and S Boccaletti. Explosive transitions to synchronization in networks of phase oscillators. *Scienti fc reports*, 3(1):1{5, 2013.

[18] Weiqing Liu, Ye Wu, Jinghua Xiao, and Meng Zhan. E ects of frequency-degree correlation on synchro-

[40]